European Journal of Haematology ISSN 0902-4441

ORIGINAL ARTICLE

CD16$^+$ CD56$^-$ NK cells in the peripheral blood of cord blood transplant recipients: a unique subset of NK cells possibly associated with graft-versus-leukemia effect

Xuzhang Lu[1], Yukio Kondo[1], Hiroyuki Takamatsu[1], Kinya Ohata[1], Hirohito Yamazaki[2], Akiyoshi Takami[3], Yoshiki Akatsuka[4], Shinji Nakao[1]

[1]Cellular Transplantation Biology, Kanazawa University Graduate School of Medical Science, Kanazawa, Ishikawa, Japan; [2]The Protected Environmental Unit, Kanazawa University Hospital, Kanazawa, Ishikawa, Japan; [3]Division of Transfusion Medicine, Kanazawa University Hospital, Kanazawa, Ishikawa, Japan; [4]Division of Immunology, Aichi Cancer Research Institute, Nagoya, Aichi, Japan

Abstract

A marked increase in CD16$^+$ CD56$^-$ NK cells in the peripheral blood (PB) was observed in a cord blood transplant (CBT) recipient with refractory acute myeloid leukaemia (AML) in association with attaining molecular remission. CD16$^+$ CD56$^-$ NK cells isolated from the patient became CD16$^+$CD56$^+$NKG2D$^+$ when they were cultured in the presence of IL-2. Although cultured CD16$^+$CD56$^-$ NK cells retained the killer-cell immunoglobulin receptor (KIR)-ligand (KIR-L) specificity and the patient's leukemic cells expressed corresponding KIR ligands, they killed patient's leukemic cells expressing ULBP2. The cytotoxicity by cultured CD16$^+$CD56$^-$ NK cells was abrogated by anti-ULBP2 antibodies. When leukemic cells obtained at relapse after CBT were examined, both the ULBP2 expression and susceptibility to the cultured NK cells decreased in comparison to leukemic cells obtained before CBT. An increase in the CD16$^+$CD56$^-$ NK cell count (0.5×10^9/L or more) in PB was observed in seven of 11 (64%) CBT recipients but in none of 13 bone marrow (BM) and eight peripheral blood stem cell (PBSC) transplant recipients examined during the similar period after transplantation. These findings suggest an increase in CD16$^+$CD56$^-$ NK cells to be a phenomenon unique to CBT recipients and that mature NK cells derived from this NK cell subset may contribute to the killing of leukemic cells expressing NKG2D ligands *in vivo*.

Key words CD56$^+$CD16$^-$ NK cell; NKG2D; graft-versus-leukemia; cord blood transplantation

Correspondence Shinji Nakao, Cellular Transplantation Biology, Kanazawa University Graduate School of Medical Science, Kanazawa University Hospital, 13-1 Takara-machi Kanazawa, Ishikawa 920-8640, Japan. Tel: +81-76-265-2274; Fax: +81-76-234-4252; e-mail: snakao@med3.m.kanazawa-u.ac.jp

Accepted for publication 6 March 2008

doi:10.1111/j.1600-0609.2008.01073.x

Cord blood transplantation (CBT) is being increasingly used for treatment of hematologic malignancies because its efficacy in the treatment of adult patients has been proven based on the findings of recent studies (1–4). One possible drawback of CBT is the less potent graft-versus-leukemia (GVL) effect than that of bone marrow transplantation (BMT) or peripheral blood stem cell transplantation (PBSCT) due to the immaturity of T cells contained in the cord blood (CB) graft (5). However, a recent study has shown the relapse rate after CBT to be comparable to that after BMT or PBSCT from human leukocyte antigen (HLA) matched sibling donors (1). Moreover, an analysis on the outcome of CBT for adult patients with acute myeloid leukaemia (AML) in Japan revealed that the rate of leukemic relapse after HLA-mismatched CBT was lower than that after HLA-matched CBT despite the fact that the incidence of graft-versus-host disease (GVHD) was similar between the two groups (Cord Blood Bank Network of Japan; unpublished observation). These clinical findings suggest that immunocompetent cells other than T cells may mediate the GVL effect after CBT.

Natural killer (NK) cells play a major role in the development of GVL effect after an HLA-mismatched stem cell transplantation (SCT) (6, 7). The GVL effect by NK cells depends on the presence of

HLA-mismatches and T cell recovery after SCT (8). Because CBT is often carried out from HLA-mismatched donors and is also associated with delayed T cell recovery (9–11), NK cells may be more likely to contribute to the development of GVL effect after CBT than after BMT or PBSCT. Few studies, however, have previously focused on the GVL effect by NK cells after CBT.

CB has a unique subset of NK cells characterized by a phenotype CD16$^+$CD56$^-$ (12–14). This NK cell subset is thought to be immature NK cells capable of differentiating into CD16$^+$CD56$^+$ NK cells (15). We recently observed an apparent increase in this NK cell subset in a patient who underwent reduced-intensity CBT for the treatment of relapsed AML after PBSCT from an HLA-compatible sibling donor. The patient achieved a molecular remission of AML in association with the NK cell increase. This observation prompted the characterization of CD16$^+$CD56$^-$ NK cells of this patient and other patients after allogeneic SCT. The present study revealed that CD16$^+$CD56$^-$ NK cells may potentially play a role in the development of the GVL effect in patients whose leukemic cells express NKG2D ligands.

Materials and methods

Patients

Peripheral blood (PB) was obtained from 11 CBT, 13 BMT (10 from related and three from unrelated donors), and eight PBSCT patients 2–135 months after transplantation. None of the patients had active graft-versus-host disease requiring corticosteroids at time of sampling or signs of infection. The original diseases of the CBT recipients included AML in four, non-Hodgkin's lymphoma (NHL) in four, myelodysplastic syndromes (MDS) in two and renal cell carcinoma in one. In the BMT recipients, those were AML in four, acute lymphoblastic leukemia (ALL) in four, MDS in three, chronic myeloid leukaemia (CML) in one, and aplastic anaemia (AA) in one while in the PBSCT recipients, those were AML in four, ALL in one, biphenotypic leukemia in two and NHL in one. All CBT recipients received an HLA-mismatched graft; the number of HLA mismatches between donor and recipient were two in seven, three in three and four in one. No HLA mismatch was observed between each donor and the BMT or PBSCT recipient except for six PBSCT recipients whose mismatches with their donors was one in two, two in one and three in one. This study was approved by our institutional review board and all patients gave their informed consent for the phenotypic and functional analyses of their peripheral blood mononuclear cells (PBMCs).

Phenotype analysis of PBMC after SCT and leukemia cells

The cell surface phenotype was determined by three-color flow cytometry. The cells were stained with various monoclonal antibodies (mAbs) specific to cell surface proteins including CD3, CD56, CD16, CD158a, CD158b (Becton Dickinson Pharmingen), NKG2A, NKG2D, NKp30, NKp44 and NKp46 (Beckman Coulter, Marseille, France). The expression of NKG2D ligands on leukemic cells from a CBT recipient was determined using mAbs specific to MICA/B (Becton Dickinson Pharmingen), ULBP1, ULBP2 and ULBP3 (R&D Systems, Minneapolis, MN).

Cell separation

PBMCs were isolated using density gradient centrifugation. NK cells were enriched by negative selection using immunomagnetic beads (Dynal NK cell isolation kit; Dynal Biotech, Lake success, NY) according to the manufacturer's recommendation (16). NK cell purity was confirmed by flow cytometry. CD16$^+$CD56$^+$ and CD16$^+$CD56$^-$ NK cells were separated from the enriched NK cells with anti-CD56-coated microBeads (MACS) by passing them through two sequential large-scale columns (Milteny Biotec, Gladbach, Germany) according to the manufacturer's instructions. CD158b$^+$ and CD158b$^-$ NK cells were separated with anti-CD158b-FITC Abs and anti-FITC microbeads.

NK cell culture

Isolated 2×10^6 CD16$^+$CD56$^+$ and CD16$^+$CD56$^-$ subsets were cultured with or without 2×10^5 irradiated (45 Gy) K562 cells transfected with the membrane-bound form of IL-15 and human 4-1BBL (K562-mb15-41BBL) kindly provided by Dr. Dario Campana of University of Tennessee College of Medicine (17) in RPMI1640 containing 10% fetal bovine serum (FBS), 50 U/mL penicillin, 50 μg/mL streptomycin and 100 IU/mL IL-2 for 14 d. The cultured NK cells were washed with RPMI1640 and then were used for the cytotoxicity assay.

Transfection of 721-221 cells with retroviral vector

An HLA class I-negative B cell line 721–221 was transfected with retrovirus vectors containing HLA-C*0301 (.221-Cw3) or HLA-C*0401 (.221-Cw4) as described previously (18). Transfectants were selected in the presence of 0.1 mg/mL neomycin and 0.1 mg/mL puromycin. The surface expression of HLA-C molecules was confirmed by flow cytometry using a mAb HLA-ABC (Immunotech, Marseille, France). A clone exhibiting the highest

level of HLA-C expression was used as a target in the cytotoxicity assay.

Cytotoxicity assay

NK cell cytotoxicity was assessed using the standard chromium release assay, as described previously (19). In blocking experiments, anti-ULBP Abs were added at 10 μg/mL to the ^{51}Cr labeled target cells and target cells were incubated at 37°C for 30 min before the addition of NK cells. The percentage of specific lysis was calculated using the formula: 100 × (count per minute [cpm] released from test sample-cpm spontaneous release)/(cpm maximum release − cpm spontaneous release).

Statistical analysis

The significance of difference in the PB $CD16^+CD56^-$ cell count between CBT recipients and recipients of BM, PBSCT, or healthy individual was assessed by Student's *t*-test. The significance of difference in the time of sampling after SCT between CBT, BMT and PBSCT was assessed by Mann-Whitney test. *P*-values < 0.05 were considered to be significant.

Results

An increase in the number of $CD16^+CD56^-$ NK cells in a CBT recipient

A 56-yr-old male (Patient 1) who relapsed with AML M0 after PBSCT from a sibling donor underwent CBT following preconditioning with fludarabin 125 mg/m^2, melphalan 80 mg/m^2, and 4 Gy TBI. The patient's leukemia was refractory to chemotherapy and there were 18% leukemic blasts in the PB at the time of preconditioning. He achieved complete chimerism in PB on day 22 after CBT. The WT1 copy number in BM RNA decreased from 13 000 copies/μg RNA before the start of preconditioning to 140 copies/μg RNA on day 60 (20). However, it rose to 1500 copies/μg RNA on day 80 after CBT. Although a molecular relapse was suspected, the WT1 copy number spontaneously decreased to 230 on day 172. Surface phenotype analysis of PB leukocytes on day 84 showed an increase in the count of $CD3^-CD16^+CD56^-$ NK cells (Fig. 1). The $CD16^+CD56^-$ NK cell count remained as high as 3.2–4.5 × 10^9/L for the following 11 months during which he remained in remission. The patient eventually relapsed with AML and died 16 months after CBT. The unexpected long term remission after reduced-intensity CBT associated with an increase in the $CD16^+CD56^-$ NK cell count prompted the characterization of the $CD16^+CD56^-$ NK cells of this patient and other patients who underwent allogeneic SCT.

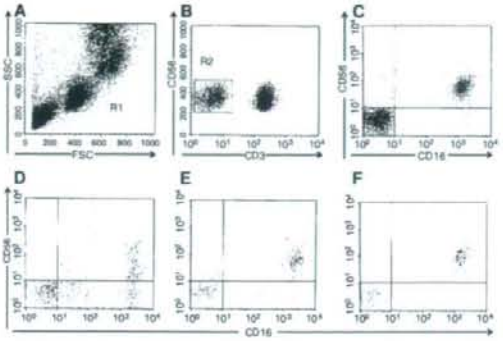

Figure 1 Phenotype of the CD16⁺ NK cells in the peripheral blood. Representative results of flow cytometry on $CD3^-$ lymphocytes from SCT recipients and healthy individuals are shown. Gates were set up to exclude any $CD3^+$ lymphocytes as shown in (A) and (B); (C) a healthy individual; (D) a CBT recipient (Patient 1); (E) a BMT recipient; (F) a PBSCT recipient.

$CD16^+CD56^-$ NK cells in PB of allogeneic SCT recipients

Because the presence of $CD16^+CD56^-$ NK cells has been reported to be characteristics of CB, the proportion of PB $CD16^+CD56^-$ NK cells as well as their absolute count was determined for other recipients of CB and the other stem cell grafts. An increase in the $CD16^+CD56^-$ NK cell count greater than 0.5 × 10^9/L was seen in seven of 11 CBT recipients but in none of 13 BMT and eight PBSCT recipients (Figs 1 and 2). There was no significant difference in the time of sampling after SCT between CBT recipients and BMT recipients ($P > 0.772$) or CBT recipients and PBSCT recipients ($P > 0.265$). Both the $CD16^+CD56^-$ NK cell proportion and the absolute count were significantly higher in CBT recipients than in other SCT recipients or in healthy individuals. In contrast, there were no significant differences in the count of other NK cell subsets including $CD56^{dim}CD16^+$ and $CD56^{bright}CD16^-$ cells among these three SCT recipient groups (data not shown). A $CD16^+CD56^-$ NK cell increase greater than 1.5 × 10^9/L was restricted to Patient 1 and another CBT recipient with NHL (Patient 2). The $CD16^+CD56^-$ NK cell counts of Patient 2, 5 months and 15 months after CBT were 1.5 × 10^9/L and 1.8 × 10^9/L, respectively.

Surface phenotype of $CD16^+CD56^-$ NK cells and leukemic cells

To characterize this unusual NK cell subset, the surface phenotype was compared between $CD16^+CD56^-$ and $CD16^+CD56^+$ NK cells from Patient 1 and Patient 2

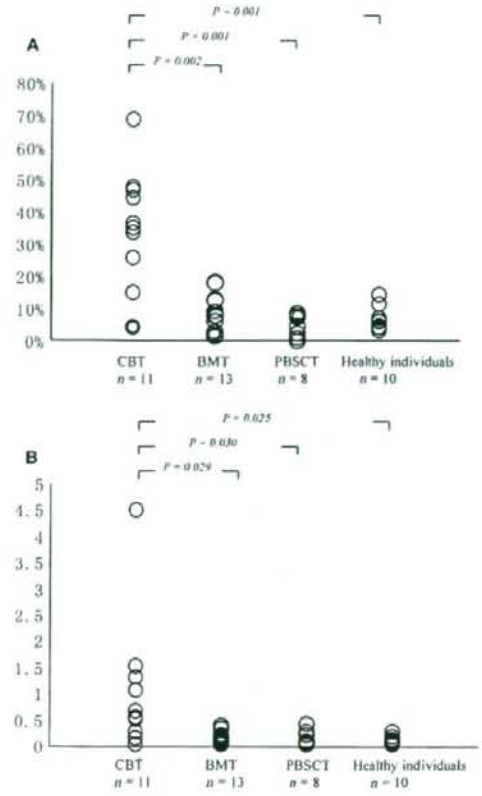

Figure 2 The proportion (A) and the absolute count (B) of $CD3^-CD16^+CD56^-$ in the PB of SCT recipients and healthy individuals. An increase in the proportion of $CD3^-CD16^+CD56^-$ NK cells (20% or more) in the PB $CD16^+$ NK cells and an increase in the absolute count of the same NK cell subset ($>0.5 \times 10^9$/L) were observed in seven of 11 CBT recipients, but in none of allogeneic 13 BM and eight PBSC transplant recipients. The $CD3^-CD16^+CD56^-$ cell count was calculated by multiplying the WBC count with the proportion (%) of this subset among the total cell event.

(Table 1). All $CD16^+CD56^-$ cells, similarly to $CD16^+CD56^+$ cells, expressed CD11a, CD18, but did not express a B-cell marker CD19, or the myeloid marker CD33 (data not shown). There were no differences in the expression levels of two major inhibitory NK receptors CD158a and CD158b between the two NK cell subsets (data not shown). On the other hand, the proportions of cells expressing activating NK receptors including NKG2D in $CD16^+CD56^-$ NK cells tended to be lower than those of $CD16^+CD56^+$ NK cells.

The leukemic cells obtained from Patient 1 before CBT exhibited an NKG2D ligand ULBP2 (Fig. 3). When the leukemic cells obtained after relapse was examined, the ULBP2 expression was observed to have decreased to levels comparable to ULBP1 and ULBP3.

Phenotypic change of $CD16^+CD56^-$ NK cells after *in vitro* culture

$CD16^+CD56^-$ NK cells derived from CB are reported to undergo differentiation *in vitro* in the presence of IL-2 (15, 21) and are therefore thought to be precursors of $CD16^+CD56^+$ NK cells (15). $CD16^+CD56^-$ NK cells were enriched from PBMCs of Patient 1 and Patient 2 and cultured in the presence of 100 IU/ml of IL-2 with or without irradiated K562-mb15-41BBL. In accordance with the results of previous studies, $CD16^+CD56^-$ NK cells from Patient 1 became $CD16^+CD56^+$ after *in vitro* culture (Fig. 4). Cultured $CD16^+CD56^-$ NK showed a tendency toward an increased expression of activating receptors including NKp30, NKp44, NKp46 and NKG2D, but did not show any changes in the expression of inhibitory receptors including CD158a, CD158b and NKG2A (Table 1).

Specificity of cultured $CD16^+CD56^-$ NK cells

Although attaining molecular remission in association with an increase in the $CD16^+CD56^-$ NK cells suggests the involvement of these NK cells in the GVL effect,

Table 1 Phenotype of the NK cell subsets from two CBT recipients

			NKp30		NKp44		NKp46		NKG2D	
			%	MFI	%	MFI	%	MFI	%	MFI
Patient 1	$CD56^+CD16^+$	Fresh	3.7	11.5	0	7.51	56.7	37.9	61.0	35.6
		Cultured	43.1	33.2	71.2	88.9	61.3	48.1	100.0	156.0
	$CD56^+CD16^-$	Fresh	0.0	8.37	0.0	7.57	17.6	12.6	46.7	12.6
		Cultured	14.2	10.4	51.4	31.0	54.2	26.8	99.9	26.8
Patient 2	$CD56^+CD16^+$	Fresh	3.6	6.71	0.0	7.72	42.9	44.3	72.3	44.3
		Cultured	14.2	39.4	51.4	49.4	54.2	54.4	99.5	54.4
	$CD56^+CD16^-$	Fresh	0.0	8.65	0.0	8.31	21.5	16.9	69.0	16.9
		Cultured	58.1	47.6	66.3	51.4	75.2	64.8	98.5	64.8

$CD16^+CD56^-$ and $CD16^+CD56^-$ NK cells were isolated from two CBT recipients and cultured with irradiated K562-mb15-41BBL in the presence of IL-2 for 14 d. Cultured NK showed increased expression of activating NK receptors including NKp30, NKp44, NKp46 and NKG2D.

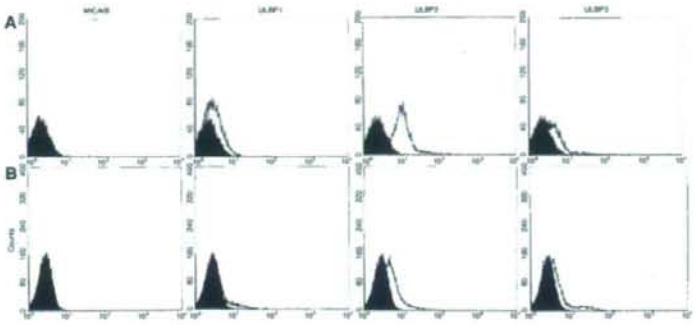

Figure 3 Expression of NKG2D ligands on leukemic cells from Patient 1. (A) leukemic cells obtained before CBT; (B) leukemic cells obtained after relapse. The proportion of ULBP2 expressing leukemic cells decreased from 59% to 9%.

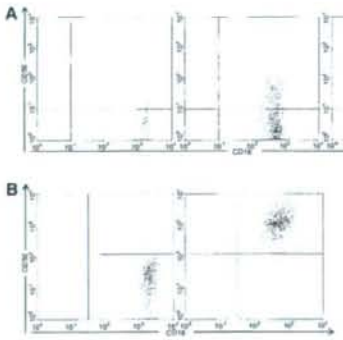

Figure 4 Phenotypic change of CD16$^+$CD56$^-$ NK cells with time associated with *in vitro* culture. Isolated CD16$^+$CD56$^-$ cells from Patient 1 were cultured in the presence of 100 IU/L IL-2 without (A) or with K562-mb15-41BBL (B). CD16$^+$CD56$^-$ NK cells from CBT recipients became CD16$^+$CD56$^+$ after the *in vitro* culture.

there was no killer-cell immunoglobulin receptor (KIR)-ligand (KIR-L) mismatch between Patient 1 and the CB donor; Patient 1 and the CB donor shared C*0102 and C*0304. To determine whether cultured NK cells derived from CD16$^+$CD56$^-$ NK cells retain specificity restricted by KIR-L of target cells, cultured NK cells from Patient 1 and Patient 2 who possessed C*0102 and C*1202 were separated into CD158b$^+$ and CD158b$^-$ NK cells, and were examined for their cytotoxicity against 721–221 cells transfected with different HLA-C alleles (Fig. 5). CD158b$^+$ NK cells failed to kill 721–221 cells transfected with HLA-C*0301 (.221-Cw3) while they killed both wild-type 721–221 cells and 721–221 cells transfected with HLA-C*0401 (.221-Cw4). Conversely, CD158b$^-$ NK cells not only killed 721–221 cells but they also killed .221-Cw3 and .221-Cw4 cells, thus indicating that the cytotoxicity due to the cultured CD158b$^+$ NK cells is inhibited by the KIR-L Cw3 of the target cells.

Cytotoxicity of cultured CD16$^+$CD56$^-$ NK cells against leukemic cells

When leukemic cells obtained from Patient 1 before CBT were used as a target, both CD158b$^+$ and CD158b$^-$ NK cells showed similar cytotoxicity to that of unfractionated NK cells (Fig. 6). The cytotoxicity was blocked by

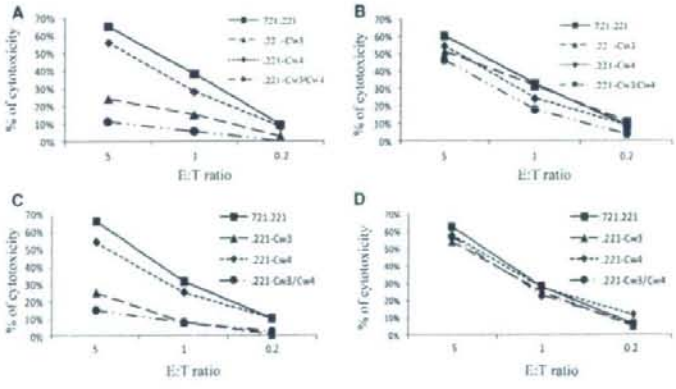

Figure 5 Specificity of NK cells derived from CD16$^+$CD56$^-$ NK cells. Cultured NK cells derived from CD16$^+$CD56$^-$ cells of Patient 1 (A and B) and Patient 2 (C and D) were separated into CD158b$^+$ (A and C) and CD158b$^-$ cells (B and D) and were examined for the cytotoxicity against 721-221 cells and 721-221 transfected with different HLA-C alleles C*0301 (.221-Cw3) and C*0401 (.221-Cw4). The data represent one of two experiments which produced similar results.

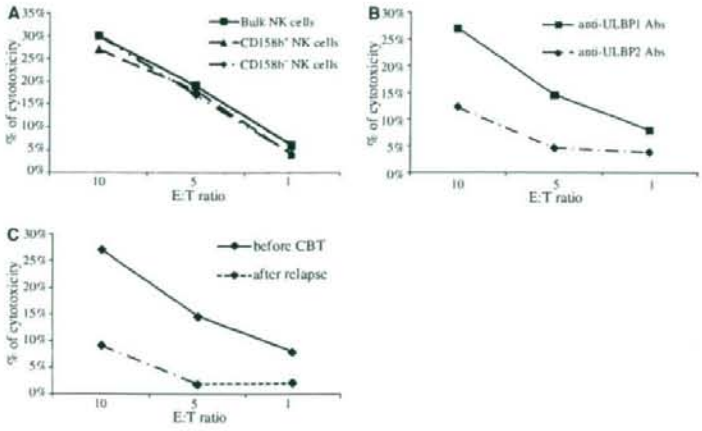

Figure 6 Cytotoxicity of cultured NK cells against leukemic cells. (A) Unseparated and separated NK cells were tested against leukemic cells obtained before CBT; (B) Leukemic cells were incubated in the presence of anti-ULBP1 or ULBP2 Abs before incubation with cultured NK cells; (C) Cytotoxicity of unseparated NK cells were tested against leukemic cells obtained before CBT or after relapse. The data represent one of three experiments which produced similar results.

treatment of leukemia cells with anti-ULPB2 mAbs. Leukemic cells obtained after relapse were relatively resistant to killing by cultured NK cells in comparison to those obtained before CBT.

Discussion

The present study revealed an increase in a unique NK cell subset characterized by CD16$^+$CD56$^-$ in CBT recipients. Although CD3$^-$CD16$^+$CD56$^-$ cells comprise monocytes, an increase in this subset was due to an increase in immature NK cells because they did not express a myeloid marker CD33 and acquired CD56 expression by *in vitro* culture in the presence of IL-2. An increase in NK cells with a similar phenotype has been shown in patients with solid tumors who were treated with IL-2 (21) and in those with HIV infection (22). Our CBT recipients did not receive cytokine therapy nor show any signs of viral infections at sampling. The expression of KIRs including CD158a and CD158b was not depressed in CD16$^+$CD56$^-$ cells of Patient 1 and Patient 2 in contrast to those of HIV patients (22). An *in vitro* culture of CD16$^+$CD56$^-$ NK cells from patients with HIV viremia in the presence IL-2 reportedly failed to induce NKp44 expression while it did induce the NKp44 expression by CD16$^+$CD56$^-$ NK cells from the two CBT recipients. It is therefore unlikely that the increase in the CD16$^+$CD56$^-$ cell count in the CBT recipients was secondary to viral infections.

Gaddy *et al.* demonstrated a novel subset of NK cells characterized by a phenotype CD16$^+$CD56$^-$ to exist in CB (12). They hypothesized that this NK cell subset represents immature NK cells capable of differentiating into CD16$^+$CD56$^+$ NK cells (15). CD16$^+$CD56$^-$ cells of our patients also underwent differentiation into CD16$^+$CD56$^+$ cells when they were cultured in the presence of IL-2. Therefore, CD16$^+$CD56$^-$ cells in PB after CBT may be derived from immature NK cells or NK precursor cells which existed in CB grafts. Previous studies on NK cells from SCT recipients and *ex vivo* engineered CB NK cells did not reveal an increased proportion of CD16$^+$CD56$^-$ cells (23–25). Both Patient 1 and Patient 2 received an HLA-mismatched CB graft although there was no KIR-L mismatch. Notably, Patient 1 had a large leukemic burden at the time of reduced-intensity preconditioning. It is therefore plausible that residual leukemic cells may have stimulated NK cell precursors to recruit CD16$^+$CD56$^-$ NK cells in Patient 1.

Patient 1's leukemic cells obtained before CBT expressed ULBP2. The incubation of CD16$^+$CD56$^-$ NK cells derived from Patient 1 in the presence of IL-2 and the K562 transfectant augmented NKG2D expression and the cultured NK cells showed cytotoxicity against leukemic cells despite that cultured NK cells retained KIR-L specificity and Patient 1's leukemic cells expressed matched KIR-L HLA-C*0304/C*0102. The cytotoxicity by the cultured NK cells decreased against leukemic cells treated with anti-ULBP2 Abs, and also against the leukemic cells obtained from Patient 1 after relapse which were devoid of ULBP2 expression. These findings suggest that mature NK cells derived from CD16$^+$CD56$^-$ NK cells may have exerted GVL effect on Patient 1's leukemic cells by way of interaction of NKG2D and ULBP2. The aberrant expression of NKG2D ligands by leukemic cells has been demonstrated by previous studies (26), but its influence on the outcome of allogeneic SCT has not yet been clarified. The results of the present study

indicate that the susceptibility of leukemic cells to NK cells may depend on both expression of NKG2D ligand on leukemic cells and the expression of NKG2D on effector NK cells. In patients with acute leukemia, leukemic cells are reported to downregulate NKp30 of autologous NK cells, thereby allowing NK cells to escape leukemic cells (27, 28). In the setting of CBT, leukemic cells expressing NKG2D ligands may tend to stimulate NK cell precursors in CB, thus inducing them to undergo differentiation.

The present study demonstrated the expansion of CD16$^+$CD56$^-$ NK cells in the PB of CBT recipients for the first time. These immature NK cells can be expanded *ex vivo* with a help of K562-mb15-41BBL cells as maintaining specificity to KIR-L and cytotoxicity against leukemic cells expressing an NKG2D ligand. Therefore, CB may be a potential source of NK cells which can be utilized for cell therapy. Further studies on a larger number of CBT recipients are needed to determine whether CD16$^+$CD56$^-$ NK cells indeed play a role in the GVL effect.

Acknowledgement

We thank Dr. Dario Campana and Dr Chihaya Imai for providing us with K562-mb15-41BBL cells.

References

1. Takahashi S, Ooi J, Tomonari A, *et al.* Comparative single-institute analysis of cord blood transplantation from unrelated donors with bone marrow or peripheral blood stem-cell transplants from related donors in adult patients with hematologic malignancies after myeloablative conditioning regimen. *Blood* 2007;**109**:1322–30.
2. Arcese W, Rocha V, Labopin M, *et al.* Unrelated cord blood transplants in adults with hematologic malignancies. *Haematologica* 2006;**91**:223–30.
3. Rocha V, Cornish J, Sievers EL, *et al.* Comparison of outcomes of unrelated bone marrow and umbilical cord blood transplants in children with acute leukemia. *Blood* 2001;**97**:2962–71.
4. Barker JN, Weisdorf DJ, DeFor TE, Blazar BR, McGlave PB, Miller JS, Verfaillie CM, Wagner JE. Transplantation of 2 partially HLA-matched umbilical cord blood units to enhance engraftment in adults with hematologic malignancy. *Blood* 2005;**105**:1343–7.
5. Harris DT, Schumacher MJ, Locascio J, Besencon FJ, Olson GB, DeLuca D, Shenker L, Bard J, Boyse EA. Phenotypic and functional immaturity of human umbilical cord blood T lymphocytes. *Proc Natl Acad Sci U S A* 1992;**89**:10006–10.
6. Ruggeri L, Capanni M, Casucci M, Volpi I, Tosti A, Perruccio K, Urbani E, Negrin RS, Martelli MF, Velardi A. Role of natural killer cell alloreactivity in HLA-mismatched hematopoietic stem cell transplantation. *Blood* 1999;**94**:333–9.
7. Ruggeri L, Capanni M, Urbani E, *et al.* Effectiveness of donor natural killer cell alloreactivity in mismatched hematopoietic transplants. *Science* 2002;**295**:2097–100.
8. Cooley S, McCullar V, Wangen R, Bergemann TL, Spellman S, Weisdorf DJ, Miller JS. KIR reconstitution is altered by T cells in the graft and correlates with clinical outcomes after unrelated donor transplantation. *Blood* 2005;**106**:4370–6.
9. Komanduri KV, St John LS, de Lima M, *et al.* Delayed immune reconstitution after cord blood transplantation is characterized by impaired thymopoiesis and late memory T cell skewing. *Blood* 2007;**110**:4543–51.
10. Giraud P, Thuret I, Reviron D, Chambost H, Brunet C, Novakovitch G, Farnarier C, Michel G. Immune reconstitution and outcome after unrelated cord blood transplantation: a single paediatric institution experience. *Bone Marrow Transplant* 2000;**25**:53–7.
11. Locatelli F, Maccario R, Comoli P, *et al.* Hematopoietic and immune recovery after transplantation of cord blood progenitor cells in children. *Bone Marrow Transplant* 1996;**18**:1095–101.
12. Gaddy J, Risdon G, Broxmeyer HE. Cord blood natural killer cells are functionally and phenotypically immature but readily respond to interleukin-2 and interleukin-12. *J Interferon Cytokine Res* 1995;**15**:527–36.
13. Bradstock KF, Luxford C, Grimsley PG. Functional and phenotypic assessment of neonatal human leucocytes expressing natural killer cell-associated antigens. *Immunol Cell Biol* 1993;**71**:535–42.
14. Phillips JH, Hori T, Nagler A, Bhat N, Spits H, Lanier LL. Ontogeny of human natural killer (NK) cells: fetal NK cells mediate cytolytic function and express cytoplasmic CD3 epsilon,delta proteins. *J Exp Med* 1992;**175**:1055–66.
15. Gaddy J, Broxmeyer HE. Cord blood CD16$^+$56$^-$ cells with low lytic activity are possible precursors of mature natural killer cells. *Cell Immunol* 1997;**180**:132–42.
16. Igarashi T, Wynberg J, Srinivasan R, Becknell B, McCoy JP Jr, Takahashi Y, Suffredini DA, Linehan WM, Caligiuri MA, Childs RW. Enhanced cytotoxicity of allogeneic NK cells with killer immunoglobulin-like receptor ligand incompatibility against melanoma and renal cell carcinoma cells. *Blood* 2004;**104**:170–7.
17. Imai C, Iwamoto S, Campana D. Genetic modification of primary natural killer cells overcomes inhibitory signals and induces specific killing of leukemic cells. *Blood* 2005;**106**:376–83.
18. Kondo E, Topp MS, Kiem HP, Obata Y, Morishima Y, Kuzushima K, Tanimoto M, Harada M, Takahashi T, Akatsuka Y. Efficient generation of antigen-specific cytotoxic T cells using retrovirally transduced CD40-activated B cells. *J Immunol* 2002;**169**:2164–71.
19. Nakao S, Takami A, Takamatsu H, *et al.* Isolation of a T-cell clone showing HLA-DRB1*0405-restricted

cytotoxicity for hematopoietic cells in a patient with aplastic anemia. *Blood* 1997;**89**:3691–9.
20. Ogawa H, Tamaki H, Ikegame K, *et al.* The usefulness of monitoring WT1 gene transcripts for the prediction and management of relapse following allogeneic stem cell transplantation in acute type leukemia. *Blood* 2003;**101**:1698–704.
21. McKenzie RS, Simms PE, Helfrich BA, Fisher RI, Ellis TM. Identification of a novel CD56$^-$ lymphokine-activated killer cell precursor in cancer patients receiving recombinant interleukin 2. *Cancer Res* 1992;**52**:6318–22.
22. Mavilio D, Lombardo G, Benjamin J, *et al.* Characterization of CD56$^-$/CD16$^+$ natural killer (NK) cells: a highly dysfunctional NK subset expanded in HIV-infected viremic individuals. *Proc Natl Acad Sci U S A* 2005;**102**:2886–91.
23. Jacobs R, Stoll M, Stratmann G, Leo R, Link H, Schmidt RE. CD16$^-$ CD56$^+$ natural killer cells after bone marrow transplantation. *Blood* 1992;**79**:3239–44.
24. Ayello J, van de Ven C, Fortino W, *et al.* Characterization of cord blood natural killer and lymphokine activated killer lymphocytes following ex vivo cellular engineering. *Biol Blood Marrow Transplant* 2006;**12**:608–22.
25. Moretta A, Maccario R, Fagioli F, *et al.* Analysis of immune reconstitution in children undergoing cord blood transplantation. *Exp Hematol* 2001;**29**:371–9.
26. Salih HR, Antropius H, Gieseke F, Lutz SZ, Kanz L, Rammensee HG, Steinle A. Functional expression and release of ligands for the activating immunoreceptor NKG2D in leukemia. *Blood* 2003;**102**:1389–96.
27. Costello RT, Sivori S, Marcenaro E, Lafage-Pochitaloff M, Mozziconacci MJ, Reviron D, Gastaut JA, Pende D, Olive D, Moretta A. Defective expression and function of natural killer cell-triggering receptors in patients with acute myeloid leukemia. *Blood* 2002;**99**:3661–7.
28. Fauriat C, Just-Landi S, Mallet F, Arnoulet C, Sainty D, Olive D, Costello RT. Deficient expression of NCR in NK cells from acute myeloid leukemia: evolution during leukemia treatment and impact of leukemia cells in NCRdull phenotype induction. *Blood* 2007;**109**:323–30.

blood

2008 112: 2160-2162
Prepublished online Jul 2, 2008;
doi:10.1182/blood-2008-02-141325

Expansion of donor-derived hematopoietic stem cells with PIGA mutation associated with late graft failure after allogeneic stem cell transplantation

Kanako Mochizuki, Chiharu Sugimori, Zhirong Qi, Xuzhang Lu, Akiyoshi Takami, Ken Ishiyama, Yukio Kondo, Hirohito Yamazaki, Hirokazu Okumura and Shinji Nakao

Blood (print ISSN 0006-4971, online ISSN 1528-0020), is published semimonthly by the American Society of Hematology, 1900 M St, NW, Suite 200, Washington DC 20036.

Brief report

Expansion of donor-derived hematopoietic stem cells with *PIGA* mutation associated with late graft failure after allogeneic stem cell transplantation

*Kanako Mochizuki,[1] *Chiharu Sugimori,[1] Zhirong Qi,[1] Xuzhang Lu,[1] Akiyoshi Takami,[1] Ken Ishiyama,[1] Yukio Kondo,[1] Hirohito Yamazaki,[1] Hirokazu Okumura,[1] and Shinji Nakao[1]

[1]Cellular Transplantation Biology, Division of Cancer Medicine, Kanazawa University Graduate School of Medical Science, Ishikawa, Japan

A small population of CD55$^-$CD59$^-$ blood cells was detected in a patient who developed donor-type late graft failure after allogeneic stem cell transplantation (SCT) for treatment of aplastic anemia (AA). Chimerism and *PIGA* gene analyses showed the paroxysmal nocturnal hemoglobinuria (PNH)–type granulocytes to be of a donor-derived stem cell with a thymine insertion in *PIGA* exon 2. A sensitive mutation-specific polymerase chain reaction (PCR)–based analysis detected the mutation exclusively in DNA derived from the donor bone marrow (BM) cells. The patient responded to immunosuppressive therapy and achieved transfusion independence. The small population of PNH-type cells was undetectable in any of the 50 SCT recipients showing stable engraftment. The de novo development of donor cell–derived AA with a small population of PNH-type cells in this patient supports the concept that glycosyl phosphatidylinositol–anchored protein–deficient stem cells have a survival advantage in the setting of immune-mediated BM injury. (Blood. 2008;112:2160-2162)

Introduction

Although small populations of CD55$^-$CD59$^-$ blood cells are often detectable in patients with aplastic anemia (AA), it remains unclear how such paroxysmal nocturnal hemoglobinuria (PNH)-type cells arise.[1] We recently encountered a patient with immune-mediated late graft failure (LGF) following allogeneic stem cell transplantation (SCT) for treatment of AA. Analyses of the patient's peripheral blood (PB) and bone marrow (BM) showed hematopoietic stem cells (HSCs) of donor origin with mutant *PIGA*, supporting the concept that glycosyl phosphatidylinositol–anchored protein (GPI-AP)–deficient stem cells have a survival advantage in the setting of immune mediated BM injury.

Methods

Patients

A 59-year-old man underwent allogeneic PBSCT from a human leukocyte antigen (HLA)–matched sibling donor after conditioning with fludarabin (120 mg/m^2), cyclophosphamide (1200 mg/m^2), and antithymocyte globulin (60 mg/kg) for treatment of very severe AA in April 2002 (Table 1) and achieved complete donor chimerism with normal blood cell counts. In January 2006, he developed pancytopenia and was diagnosed as having LGF without residual recipient cells. The patient underwent a second PBSCT from the original donor without preconditioning on February 8, 2006. Pancytopenia resolved completely by day 16 after PBSCT. However, at approximately day 60, the blood counts decreased gradually, and the patient became transfusion-dependent. On day 196 after the second PBSCT, the white blood cell (WBC) count was 5.3×10^9/L with 17% neutrophils, the hemoglobin concentration was 75 g/L, and the platelet count was 22×10^9/L. Treatment with horse antithymocyte globulin (ATG) and cyclosporine was started on day 205 after the second PBSCT. Transfusions were terminated after 88 days of the immunosuppressive therapy. Although the patient presently receives low-dose tacrolimus for treatment of chronic graft-versus-host disease, which developed 1 year after the second PBSCT, his pancytopenia has markedly improved as shown in Table 1. PB and BM of the patient were subjected to analyses of chimerism and flow cytometry to detect CD55$^-$CD59$^-$ cells and *PIGA* gene analysis.

As controls, the PB from 51 SCT recipients (48 with hematologic malignancies and 3 with AA) who achieved a complete recovery of donor-derived hematopoiesis were subjected to flow cytometric analysis for the screening of CD55$^-$CD59$^-$ cells. Of the 51 patients, 4 and 23, respectively, had acute graft-versus-host disease (GVHD) of grade II or higher and chronic GVHD at sampling.

BM aspirates were obtained from the patient's donor and 10 healthy individuals for *PIGA* gene analysis. Informed consent was obtained from all patients and healthy individuals in accordance with the Declaration of Helsinki for blood examination, and the experimental protocol for *PIGA* gene analysis was approved by our participating institutional ethics committee (No.157).

Detection of PNH-type cells

To detect GPI-AP deficient (GPI-AP$^-$), PNH-type cells, we performed high-sensitivity 2-color flow cytometry of granulocytes and red blood cells (RBCs), as described previously.[1] The presence of 0.003% or more CD55$^-$CD59$^-$CD11b$^+$ granulocytes and 0.005% or more CD55$^-$CD59$^-$ glycophorin-A$^+$ RBCs was defined as an abnormal increase based on the results in 183 healthy individuals.[2]

Cell sorting and chimerism analysis

CD3$^+$ cells were isolated from the PB mononuclear cells of the patient using magnetic-activated cell sorting (MACS) CD3 Microbeads (Miltenyi Biotec, Auburn, CA). The CD55$^-$CD59$^-$CD11b$^+$ granulocytes were separated from the CD55$^+$CD59$^+$CD11b$^+$ granulocytes with a cell sorter (JSAN; Bay Bioscience, Yokohama, Japan). More than 95% of the sorted cells were

Submitted February 21, 2008; accepted June 17, 2008. Prepublished online as *Blood* First Edition paper, July 2, 2008; DOI 10.1182/blood-2008-02-141325.

*K.M. and C.S. contributed equally to this work.

The online version of this article contains a data supplement.

The publication costs of this article were defrayed in part by page charge payment. Therefore, and solely to indicate this fact, this article is hereby marked "advertisement" in accordance with 18 USC section 1734.

Table 1. Hematologic parameters of donor and recipient

	Donor		Recipient			
			Before 1st SCT	Before 2nd SCT	At ATG therapy	After 20 mo of ATG therapy
Date	Apr 2002	May 2008	Apr 2002	Jan 2006	Aug 2006	Apr 2008
WBC count, $\times 10^9$/L	7.0	5.1	1.2	1.7	5.3	4.0
Neutrophil proportions, %	77	65	0	0	17	62
RBC count, $\times 10^{12}$/L	4.21	4.43	2.20	2.75	2.07	3.04
Reticulocytes, 10^9/L	not tested	35	2	3	26	61
Hemoglobin, g/L	146	150	72	89	75	120
Platelet count, 10^9/L	261	230	19	52	22	54

$CD55^-CD59^-CD11b^+$. The *D1S80* locus was amplified from DNA of different cell populations with an AmpliFLP D1S80 PCR Amplification Kit (Perkin-Elmer Cetus, Norwalk, CT).

PIGA gene analysis

The coding regions of *PIGA* were amplified by seminested PCR or nested PCR from DNA extracted from the sorted PNH-type cells using 12 primer sets[3,4] (Table S1, available on the *Blood* website; see the Supplemental Materials link at the top of the online article), and 6 ligation reactions were used to transform competent *Escherichia coli* JM109 cells (Nippon Gene, Tokyo, Japan). Five clones were selected randomly from each group of transfectants and subjected to sequencing with a BigDye Terminator v3.1 Cycle Sequencing Kit (Applied Biosystems, Foster City, CA) and an ABI PRISM 3100 Genetic Analyzer (Applied Biosystems).

Amplification refractory mutation system PCR

On the basis of a mutant sequence detected in *PIGA* of the patient, a nested amplification refractory mutation system (ARMS) forward primer with a 3′-terminal nucleotide sequence complementary to the mutant sequence was prepared[3] (Table S1). To enhance the specificity, a mismatch at the penultimate nucleotide position of the mutation site was incorporated in the ARMS forward primer (P1).[6,7] P1 and a reverse primer (P3) were used to amplify a 127 bp fragment containing the mutant sequence from the exon 2 amplified product. PCR was conducted under the following conditions: denaturation for 30 seconds at 94°C, annealing for 60 seconds at 64°C and extension for 90 seconds at 72°C for 20 cycles. Another forward primer (P2), complementary to the wild-type *PIGA* sequence upstream of the mutation site, was used in combination with P3 to amplify an internal control according to the same condition of ARMS-PCR.

Results and discussion

PNH-type cells were not detected in the donor or the patient at the time of development of the first LGF, whereas 0.147% PNH-type granulocytes and 0.019% PNH-type RBCs were detected in the PB

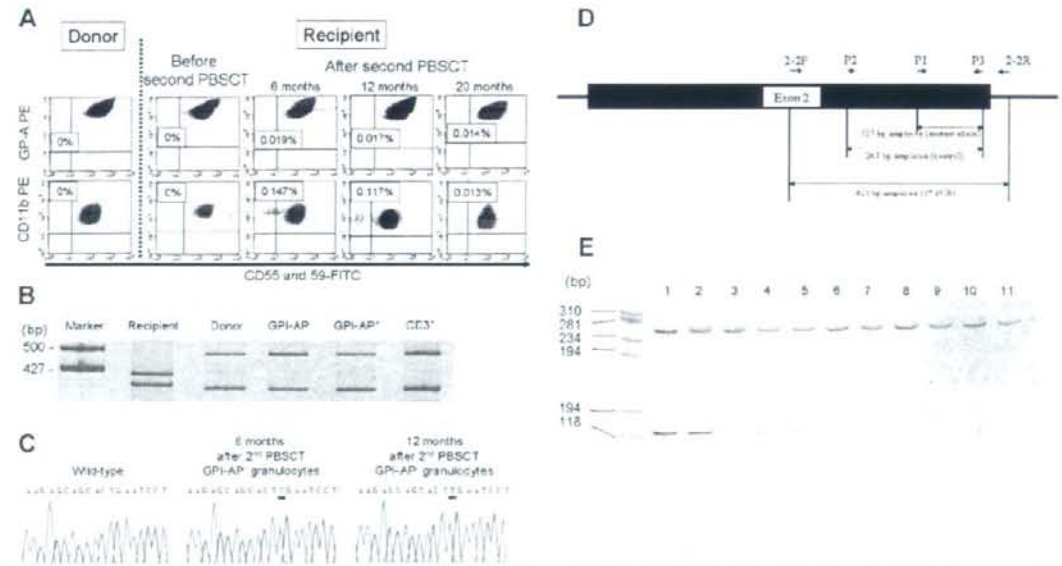

Figure 1. Analysis of PNH-type cells after the second PBSCT. (A) High-sensitivity flow cytometry detected small populations of $CD55^-CD59^-$ cells in both granulocytes and red blood cells at the development of the second LGF as well as in those obtained 6 and 12 months later, but did not detect PNH-type cells in the donor or in the recipient before the second PBSCT. The numbers denote the proportion of PNH-type cells in $CD11b^+$ granulocytes or glycophorin A^+ RBCs. (B) *D1S80* allelic patterns of sorted $GPI\text{-}AP^-$ granulocytes, $GPI\text{-}AP^+$ granulocytes, and $CD3^+$ lymphocytes. The polymerase chain reaction (PCR) products were subjected to 8% polyacrylamide gel electrophoresis and visualized by silver staining. (C) Nucleotide sequences of *PIGA* exon 2 in DNA from PNH-type granulocytes obtained 6 and 12 months after the second PBSCT. (D) A schematic illustration for ARMS-PCR is shown. Primer positions for the first, second are shown by short arrows. A black box and adjacent lines represent exon 2 and introns, respectively. (E) Amplified products of control PCR (the upper gel) and ARMS-PCR (the lower gel) were electrophoresed in 12.5% polyacrylamide gel and visualized by the silver staining. A pMD20-T vector containing the mutated exon 2 fragment was used as a positive control for ARMS-PCR. The template DNA derives from a plasmid containing the mutated exon 2 in lane 1, donor BM in lane 2, donor PB in lane 3, recipient BM in lane 4, recipient PB in lane 5, and BM from healthy individuals in lanes 6 to 11. PCR with a 5′ primer specific to the nucleotide sequence upstream of the mutated sequence amplified a 261 bp fragment from DNA of the donor and all healthy individuals.

obtained at the time of development of the second LGF (Figure 1A). Similar percentages of PNH-type blood cells were detectable in the PB of the patient 6 and 14 months later. When PB from 51 SCT recipients was examined, none of the patients were found to have detectable PNH-type cells (data not shown). PNH-type blood cells were also undetectable in a donor PB sample obtained 21 months later.

The *D1S80* locus allelic pattern of the PNH-type granulocytes in the patient was compatible to that of the donor (Figure 1B). The emergence of donor-derived PNH-type cells and hematologic improvement after immunosuppressive therapy suggest that LGF arises as a result of de novo development of AA which affects the donor-derived hematopoietic stem cells (HSCs).

PIGA gene analysis of the DNA prepared from the sorted PNH-type cells of the patient obtained at the development of LGF and 6 months later showed an insertion of thymine at position 593 (codon 198) in 3 of 5 clones and 5 of 5 clones examined, respectively (Figure 1C). Mutations in other exons were not identified. The presence of a single *PIGA* mutation in PNH-type granulocytes and its persistence over 6 months suggest that these PNH-type cells are derived from a mutant HSC rather than from a committed granulocyte progenitor cell. Moreover, an ARMS-PCR with a 5′ primer specific to the mutated sequence amplified a 127 bp fragment from DNA of the donor BM as well as of the recipient BM and PB while it failed to amplify the same fragment in donor PB and in BM of all 10 healthy individuals (Figure 1D).

These experiments demonstrate that *PIGA*-mutant HSCs were present in the BM of the donor in a dormant state and were transplanted into the recipient and provide, for the first time, in vivo evidence that *PIGA* mutant, GPI-AP–deficient HSCs have a survival advantage in the setting of immune mediated BM injury. Similarly, relative resistance to immune injury likely accounts for the high incidence of PNH observed in association with acquired AA.

Acknowledgments

We thank Ms Shizuka Yasue, Ms Megumi Yoshii, and Ms Rie Oumi for their excellent technical assistance. We also thank Dr Charles Parker for his critical reading of this manuscript.

This work was supported by a Grant-in-Aid for Scientific Research from the Ministry of Education, Culture, Sports, Science and Technology of Japan (No.15390298), a grant from the Ministry of Health, Labour and Welfare of Japan, and a grant from the Japan Intractable Diseases Research Foundation.

Authorship

Contribution: K.M. and C.S. participated in designing and performing the research. Z.Q. and X.L. performed experiments. K.M., C.S., and S.N. wrote the paper. C.S., A.T., K.I., Y.K., H.Y., and H.O. provided patient care. All authors have approved the final version of the manuscript.

Conflict-of-interest disclosure: The authors declare no competing financial interests.

Correspondence: Shinji Nakao, Cellular Transplantation Biology, Division of Cancer Medicine, Kanazawa University Graduate School of Medical Science, 13-1 Takaramachi, Kanazawa, Ishikawa 920-8641, Japan; e-mail: snakao@med3.m.kanazawa-u.ac.jp.

References

1. Sugimori C, Chuhjo T, Feng X, et al. Minor population of CD55-CD59- blood cells predicts response to immunosuppressive therapy and prognosis in patients with aplastic anemia. Blood. 2006;107:1308-1314.
2. Sugimori C, Yamazaki H, Feng X, et al. Roles of DRB1 *1501 and DRB1 *1502 in the pathogenesis of aplastic anemia. Exp Hematol. 2007;35:13-20.
3. Kai T, Shichishima T, Noji H, et al. Phenotypes and phosphatidylinositol glycan-class A gene abnormalities during cell differentiation and maturation from precursor cells to mature granulocytes in patients with paroxysmal nocturnal hemoglobinuria. Blood. 2002;100:3812-3818.
4. Mortazavi Y, Merk B, McIntosh J, et al. The spectrum of PIG-A gene mutations in aplastic anemia/paroxysmal nocturnal hemoglobinuria (AA/PNH): a high incidence of multiple mutations and evidence of a mutational hot spot. Blood. 2003;101:2833-2841.
5. Newton CR, Graham A, Heptinstall LE, et al. Analysis of any point mutation in DNA. The amplification refractory mutation system (ARMS). Nucleic Acids Res. 1989;17:2503-2516.
6. Dang RK, Anthony RS, Craig JI, Leonard RC, Parker AC. Limitations of the use of single base changes in the p53 gene to detect minimal residual disease of breast cancer. Mol Pathol. 2002;55:177-181.
7. Bai RK, Wong LJ. Detection and quantification of heteroplasmic mutant mitochondrial DNA by real-time amplification refractory mutation system quantitative PCR analysis: a single-step approach. Clin Chem. 2004;50:996-1001.

European Journal of Haematology ISSN 0902-4441

ORIGINAL ARTICLE

Aberrant increase in the immature platelet fraction in patients with myelodysplastic syndrome: a marker of karyotypic abnormalities associated with poor prognosis

Naomi Sugimori[1], Yukio Kondo[1], Masami Shibayama[2], Mika Omote[2], Akiyoshi Takami[3], Chiharu Sugimori[1], Ken Ishiyama[1], Hirohito Yamazaki[1], Shinji Nakao[1]

[1]Cellular Transplantation Biology, Division of Cancer Medicine, Kanazawa University Graduate School of Medical Science; [2]Department of Clinical Laboratory, Kanazawa University Hospital; [3]Division of Transfusion Medicine, Kanazawa University Hospital, Kanazawa, Japan

Abstract

Objectives: Some patients with myelodysplastic syndrome (MDS) show a marked increase in the percentage of immature platelet fraction (IPF%) despite the absence of severe thrombocytopenia. To determine the significance of such an unbalanced increase in the IPF%, we investigated the IPF% and other laboratory findings of 51 patients recently diagnosed with MDS. *Method:* Subjects consisted of 80 healthy males, 90 healthy females, and 51 patients with MDS and 20 patients with idiopathic thrombocytopenic purpura (ITP). The IPF and IPF% were determined using a Sysmex XE-2100 system loaded with IPF Master software (XE IPF Master, Sysmex). Platelet counts were measured simultaneously. *Results:* IPF% and platelet counts of these patients ranged from 1.1% to 25.1% (median, 5.3%) and from 6 to 260 $\times 10^9$/L (median, 71 $\times 10^9$/L), respectively. Twelve patients showed platelet counts more than 50 $\times 10^9$/L with 10% or more IPF%. All of the 12 patients had chromosome abnormalities including monosomy 7 and complex abnormalities involving 7 or 5q. In the other 39 patients who did not show the aberrant IPF% increase, chromosomal abnormalities were seen only in seven patients and none of them had chromosome 7 abnormalities. The IPF% of two patients increased to more than 10% in association with the appearance of monosomy 7. *Conclusions:* These findings suggest that a high IPF% in MDS patient may be a marker for karyotypic abnormalities with a poor prognosis, including chromosome 7 abnormalities.

Key words immature platelet fraction; IPF%; monosomy 7; myelodysplastic syndromes; Sysmex XE2100

Correspondence Shinji Nakao, MD, PhD, 13-1 Takaramachi, Kanazawa, Ishikawa, Japan, 920-8640. Tel: 81 76 265 2274; Fax: 81 76 234 4252; e-mail: snakao@med3.m.kanazawa-u.ac.jp

Accepted for publication 11 September 2008

doi:10.1111/j.1600-0609.2008.01156.x

Reticulated platelets are RNA-rich immature platelets and are thought to reflect the ability of bone marrow to produce platelets (1). Reticulated platelets can be measured by flow cytometry using thiazole orange (2). However, the measurement of the reticulated platelets has not been included in routine examinations because of the complexity of the procedure. Furthermore, the standard method for measurement of reticulated platelets has not been established so far. Some assays use whole blood and others use platelet-rich plasma. Monoclonal antibodies specific to platelets used to delineate reticulated platelets are varying and normal counts of reticulated platelets are reported to vary from 1% to 20% (2–16).

A recent software program using the Sysmex XE2100 fully automated complete blood count analyzer (Sysmex, Kobe, Japan) has facilitated the measurement of RNA-rich immature platelets automatically. Although this instant assay lacks specificity, the measurement of the immature platelet fraction percentage in total platelets (IPF%) may be useful in ascertaining whether thrombocytopenia is caused by reduced platelet production or increased metabolic turnover because of platelet destruction. Indeed, IPF% has been successfully utilized to differentiate ITP and aplastic anemia (AA) (17).

The measurement of IPF% has also been shown to be useful in predicting platelet recovery following

myelosuppression because of chemotherapy or preconditioning for stem cell transplantation (18–21). However, few studies have focused on the clinical significance of measuring IPF% in patients with myelodysplastic syndrome (MDS).

High IPF% is usually seen in thrombocytopenic patients whose thrombopoiesis is accelerated to compensate for low platelet counts. However, some patients with MDS exhibit IPF% above 10% despite the fact that there is no or only mild thrombocytopenia. All of the first three MDS patients we observed with such an aberrant feature had chromosome 7 abnormalities and rapidly progressed to acute myeloid leukemia. We therefore hypothesized that the unbalanced increase in IPF% may represent aberrant thrombopoiesis in MDS patients with a poor prognosis. To characterize patients with MDS showing aberrantly high IPF%, we retrospectively studied IPF% and other laboratory data in 51 patients recently diagnosed with MDS and in other patients with thrombocytopenia.

Design and methods

Subjects

Subjects consisted of 80 healthy males ranging in age from 23 to 63 yr, 90 healthy females ranging in age from 21 to 56 yr, and 51 patients with MDS and 20 patients with ITP. All subjects underwent the IPF measurement at our hospital and were subsequently followed. According to the FAB classification of MDS, 35 patients had refractory anemia (RA), one patient had RA with ringed sideroblasts (RARS), 12 patients had refractory anemia with excess blasts (RAEB) and three patients had chronic myelomonocytic leukemia. All patients and healthy individuals provided oral informed consent to the measurement of IPF.

Measurement of IPF

The IPF and IPF% were determined using a Sysmex XE-2100 system loaded with IPF Master software (XE IPF Master, Sysmex). XE-2100 is a fully automated analyzer that aspirates and analyzes ethylenediaminetetraacetic acid blood samples, and prints out test results all in about 1 min. IPF and reticulocytes were stained using reticulocyte reagents (polymethylene and oxazine dyes) and then measured by flow cytometry using a semiconductor laser. A computer algorithm discriminates the mature and immature platelets by the intensity of forward scatterd light and fluorescence. Mature platelets appear as blue dots and the immature platelets are displayed as green dots, the latter constituting the IPF parameter. IPF is calculated as the ratio of immature platelet to the total number of platelets (17, 19). When the fluorescent intensity (nucleic acid content) and the forward-scattered light intensity (Forward Scatter reflecting cell size) were plotted on the X and Y axes, respectively, the RNA-rich IPF appears in the green area on the two dimensional scattergram (Fig. 1). Platelet counts were measured simultaneously.

Cytogenetic and morphological analyses

On the day of peripheral blood collection or within 1 month before or after blood collection, karyotype analyses of bone marrow aspirates based on G banding or fluorescence *in situ* hybridization (FISH) were performed. Peripheral blood and bone marrow smears were analyzed under microscopy to ascertain the morphological characteristics of platelets and megakaryocytes.

Statistical analysis

The differences between the two groups were evaluated by Student's *t*-test. The relationship between IPF% and the platelet count was estimated using the simple linear regression and correlation analyses. Survival probabilities were estimated by the Kaplan–Meier method, and the differences in survival distributions were evaluated by log-rank test.

Results

Platelet count and IPF

Platelet counts for the control group (healthy males and females) ranged from 162 to 347 $\times 10^9$/L (median:

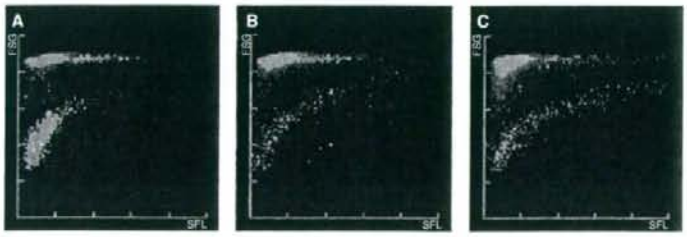

Figure 1 Measurement of immature platelet fraction (IPF). Examples of IPF scattergrams are shown. (A) a healthy individual with normal IPF%; (B) idiopathic thrombocytopenic purpura patient with IPF% of 19.8%; (C) myelodysplastic syndrome patient with IPF% of 29%. The green area indicates the IPF whereas the blue one indicates mature platelets.

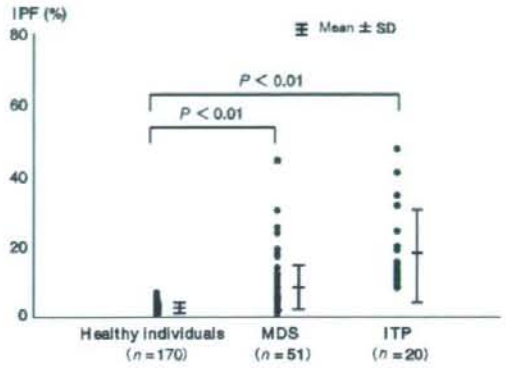

Figure 2 Immature platelet fraction (IPF) % in healthy individuals and patients with thrombocytopenia. IPF% values as determind by the blood analyzer are plotted for healthy individuals, patients with myelodysplastic syndrome and patients with idiopathic thrombocytopenic purpura.

237×10^9/L), compared with 2 to 49×10^9/L for ITP patients (median: 21×10^9/L) and from 6 to 297×10^9/L for MDS patients (median: 73×10^9/L). The mean (±SD) IPF% for the control group was 2.07 ± 1.06%, while the values for the other groups were significantly higher, at 8.80 ± 8.09% for MDS patients and 18.1 ± 11.5% for ITP patients ($P < 0.01$) (Fig. 2). IPF% was normal (0.51–4.72%) in 19 of the 51 MDS patients while 16 patients showed > 10% IPF%. Of these 16 patients, 12 patients had $\geq 50 \times 10^9$/L platelets.

Correlation between IPF% and platelet count

The correlation between IPF% and platelet count was examined for healthy individuals, ITP and MDS patients (Fig. 3). There was an inverse relationship between the two parameters in healthy individuals and ITP patients, but not in MDS patients. Some MDS patients (inside the ellipse) displayed high IPF% despite the presence of normal platelet counts. There was no apparent difference in the IPF distribution on scattergram between ITP and MDS patients with high IPF% (Fig. 1).

Clinical features of patients with platelet counts $\geq 50 \times 10^9$/L and IPF% ≥10% (Table 1)

Clinical features were compared between 12 patients with $\geq 50 \times 10^9$/L platelet count and ≥10% IPF% (high IPF% patients) and those who do not meet these criteria (control patients). Chromosomal abnormalities were found in all of the 12 high IPF% patients, but in only seven of the 39 control patients. There were no differences in age, gender, WBC, Hb, platelet count, or the proportion of advanced MDS (RAEB) between the two groups. Table 1 shows the clinical characteristics of these 12 patients. Notably five patients had monosomy 7, and another patient had complex abnormalities involving chromosome 7. Three patients showed complex abnormalities including 5q deletion. Chromosomal abnormalities in the control patients were trisomy 8 in two, 20q deletion in one, 5q deletion in one, trisomy 9 in one, 48, XY +Y,+Y in one and 47, XY, del(20)(q11),+21 in one. The patient in the control group showing only 5q deletion also showed a normal platelet count (140×10^9/L) and low IPF% (2.5%).

Morphological examination of blood and bone marrow smears showed marked variation in the platelet size in six of 12 (50%) patients and a ratio of 10% or more micro or small megakaryocytes to total megakaryocytes in 10 of 12 (83%) of the high IPF%

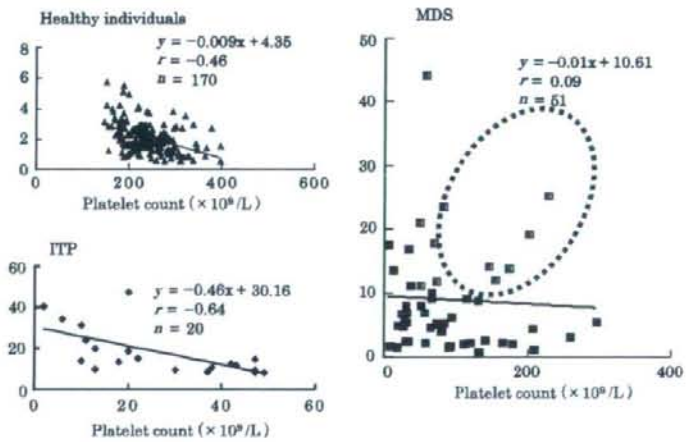

Figure 3 Correlation between immature platelet fraction (IPF) % and platelet count. IPF% and platelet count of the three different groups are plotted. X axis, platelet count; Y axis IPF%. The dotted ellipse denotes samples showing an aberrant correlation. The patients showing aberrant IPF% with higher platelet are depicted in red.

Table 1 Clinical features of patients with platelet count ≥50 × 10^9/L and IPF% ≥10%

	Case	Age/ sex	IPF%	Platelet count (×10^9/L)	Chromosomal aberration	WHO classification IPSS
1	RAEB	70 F	44.1	57	46,XX,del(1)(p),del(5)(q) 18/20 46,XX 2/20	RAEB 1 Int-2
2	RA	59 M	29.0	50	44,XY,add(1)(q32),add(5)(q11.2),add(6)(p21), −7,−8,9,add(9)(q22),10,add(11)(q23),add(12)(p11.2),add(14)(q32),−17, add(17)(q21),+mar1, +mar2, +mar3	RCMD Int-2
3	RAEB	51 F	25.1	229	46,XX, −1, add(4)(q21), −5, der(7)add(7)(p22)del(7)(q32), −11, +3mar 11/20 92,XXXX, −1, −1, add(4)(q21)×2, −5, −5, der(7)add(7)(p22)del(7)(q32) ×2, −11, −11, +6mar 1/20 46,XX 8/20	RCMD Int-2
4	RA	71 F	23.5	82	44,XX,add(5)(q11), add(6)(q13), −7, add(11)(q11), −12, del(16)(p11), −17, −17, del(20)(q11), +2mar 14/20 46,XX 6/20	RCMD Int-2
5	RARS	65 F	20.9	50	45, XX, der(3;12)(q10;10), del(5)(q13q31), −18, add(18)(p11), −20, +21, +22 5/2 47, XX, del(5)(q13q31), −18, add(18)(p11), +19, −20, +22, +mar 9/20 46, XX 6/20	RCMD-RS Int-2
6	RA	77 M	19.0	204	45, XY, −7 15/20 46, XY 5/20	RA Int-1
7	RA	80 M	14.0	147	46, XY, del(5)(q) 4/20 46, XY, del(5)(q), del(20)(q11.2q13.3) 3/20 46, XY 13/2	RCMD Int-1
8	RAEB	67 M	13.7	175	44, XY, add(5)(q11), −7, add(12)(p11), −18 1/20 44, XY, add(5)(q11), −7, add(8)(p11), add(12)(p11), −18 12/20 44, XY, add(5)(q11), −7, add(12)(p11), der(15;17)(q10;q10), −18, +mar 2/20 45, XY, add(5)(q11), −7, add(12)(p11), −18, +mar 3/20 46, XY 2/20	RAEB-1 Int-2
9	RAEB	52 M	12.1	51	45, XY, add(5)(q11), −7, add(17)(p11), −20, del(22)(q11), +mar 4/20 45, XY, add(5)(q11), −7, add(17)(p11), add(20)(q13), del(22)(q11), +mar 1/20 45, XY, add(5)(q11), −7, add(17)(p11), −18, add(20)(q13), del(22)(q11), +mar 1/20 43, XY, dic(3;14)(p11;p11),add(5)(q11), −7, add(17)(p11), −20, −22, +mar 1/20 46, XY 13/20	RCMD Int-1
10	RAEB	59 F	11.9	156	45, XX, −18, +mar 20/20	RAEB-1 Int-1
11	RA	78 F	11.8	73	45,X,-X 20/20	RCMD Int-1
12	RA	60 M	11.1	50	46,XY, add(12)(p11) 20/20	RCMD Int-1

patients. These abnormalities were found only in four of the 39 (10%) control patients. The mean platelet distribution width (PDW), an indicator of variability in platelet particle size distribution and mean platelet volume (MPV) were evaluated in 34 patients with MDS. These values were significantly higher in the high IPF% group than in the control group (PDW, 20.2 fl vs. 11.3 fl and MPV, 12.0 fl vs. 10.2 fl), suggesting the presence of prominent dysthrombopoiesis in MDS patients with high IPF%.

Change in IPF% associated with the appearance of chromosome 7

Two patients with RA showed changes in IPF% over the observation period in this study. In one patient who showed a gradual increase in the IPF%, monosomy 7 newly appeared, and the patient's RA subsequently evolved into RAEB (Fig. 4a). In another patient who responded to metenolone acetate and menatetrenone, IPF% gradually decreased from 29.0% to 9.0% in association with a decrease in the percentage of monosomy 7

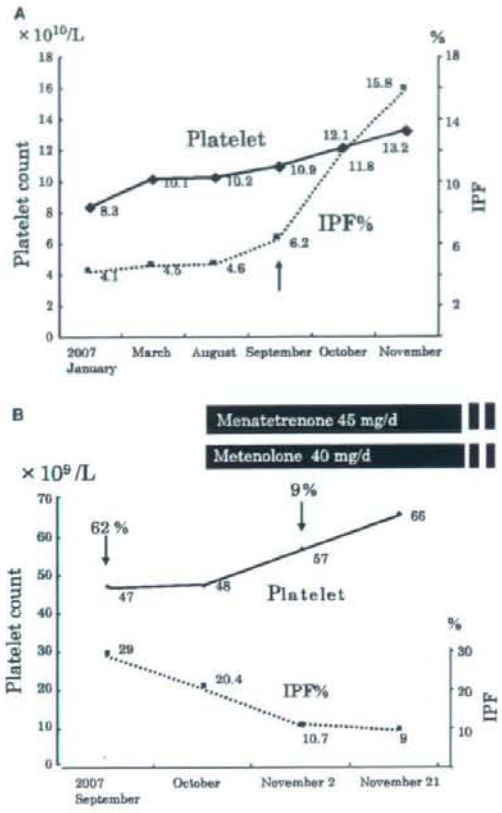

Figure 4 Changes in immature platelet fraction (IPF) % associated with the emergence or decrease of monosomy 7 clones. (A) A 22-yr-old woman with RA who originally had chromosome abnormalities, including der(1;18) showed an increase in IPF% when a monosomy 7 clone appeared. The arrow indicates the time when the monosomy 7 was first detected. (B) A 59-yr-old man with RCMD (case 2 in Table 1) with complex chromosome abnormalities including monosomy 7 who showed a decrease in IPF% in association with an improvement of pancytopenia after treatment with metenolone acetate and menatetrenone. The ratio of monosomy 7 clones as determined by FISH at the times indicated by the arrows showed a decrease from 62% to 9%.

clone from 62% to 9.2% as demonstrated by FISH analysis (Fig. 4b).

Relationship of high IPF% with prognosis

The overall survival rate was compared between the high IPF% group and the control group. As shown in Fig. 5, the patients with high IPF% show a lower survival rate than the control patients although the difference was not significant.

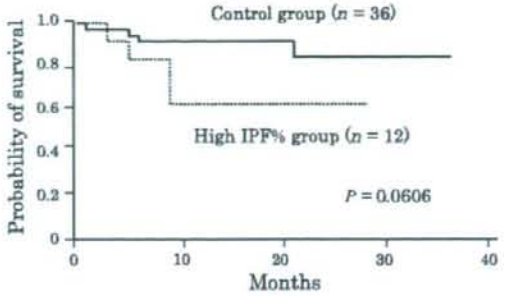

Figure 5 Kaplan–Meier analysis of the probability of overall survival (OS) in patients with myelodysplastic syndrome. OS was defined as the interval from the day of first measurement of IPF% to death or the last examination.

Discussion

IPF% has been successfully used for discrimination of pathophysiologies underlying thrombocytopenia (17, 18). Few studies, however, focused on IPF% in patients with MDS. The present study showed significantly higher IPF% in MDS patients than in healthy individuals, though there was a great range of IPF% values in MDS patients. In keeping with previous reports showing that a high IPF% reflects accelerated thrombopoiesis, there was an inverse correlation between IPF% and the platelet count in healthy individuals or that in patients with ITP. In contrast, some MDS patients showed a positive correlation between IPF% and the platelet count. Moreover, all patients with a high IPF% and a platelet count $> 50 \times 10^9$/L showed chromosomal abnormalities including chromosome 7 abnormalities. The absence of monosomy 7 or chromosome 7 abnormalities in the other 39 patients suggests that an aberrant increase in IPF% represents a marker for the presence of chromosomal abnormalities with poor prognosis. The increase in IPF% in association with the emergence the monosomy 7 in one patient and a decrease in IPF% associated with a decrease in the monosomy 7 clone in another patient support this hypothesis.

Most patients with high IPF% showed marked high platelet size variation, and both MPV and PDW in these patients tended to be higher than those in MDS patients without high IPF as well as in healthy adults. The signs of dysmegakaryopoiesis such as micromegakaryocytes and isolated multinucleated megakaryocytes were commonly seen in MDS patients with high IPF%. Thus, the aberrantly high IPF% in MDS patients probably reflects the presence of dysthrombopoiesis. A recent report by Dolan *et al.* revealed prominent dysmegakaryopoiesis in patients with monosomy 7. This may account for the high incidence of monosomy 7 in patients with high IPF% (22).

According to the international prognostic scoring system (IPSS), all MDS patients with ≥20% IPF were classified as Int-2 (Table. 1), and the overall survival of high IPF% patients tended to be lower than that of control patients (Fig. 5). It is therefore possible that low-risk MDS patients considered at low risk according to IPSS may actually be at high risk for progression to leukemia if IPF% is high. IPF% can be measured very quickly using a fully automated blood cell analyzer. An increase in IPF% could be the first sign of developing 7 monosomy in patients being followed up for low-risk MDS or AA. Thus, incorporating IPF assessment into the routine examination of patients with bone marrow failure as well as in the general check-ups for healthy individuals may be useful for early identification of MDS patients with poor prognosis. Our findings warrant a prospective clinical study on MDS patients to ascertain the significance of IPF% in the management of MDS.

Acknowledgements

We thank Ms Chiaki Tanaka and her colleagues of SYSMEX CORPORATION Scientific Affairs for their technical assistance.

References

1. Ingram M, Coopersmith A. Reticulated platelets following acute blood loss. *Br J Haematol* 1969;**17**:225–9.
2. Kienast J, Schmitz G. Flow cytometric analysis of thiazole orange uptake by platelets: a diagnostic aid in the evaluation of thrombocytopenic disorders. *Blood* 1990;**75**:116–21.
3. Consolini R, Calleri A, Bengala C, Legitimo A, Conte FP. Evaluation of thrombopoiesis kinetics by measurement of reticulated platelets and CD34(+) cell subsets in patients with solid tumors following high dose chemotherapy and autologous peripheral blood progenitor cell support. *Haematologica* 2001;**86**:959–64.
4. Ault KA, Rinder MH, Mitchell J, Carmody BM, Vary PC, Hillman SR. The significance of platelets with increased RNA content (reticulated platelets). A measure of the rate of thrombopoiesis. *Am J Clin Pathol* 1992;**98**:637–46.
5. Watanabe K, Takeuchi K, Kawai Y, Ikeda Y, Kubota F, Nakamoto H. Automated measurement of reticulated platelets in estimating thrombopoiesis. *Eur J Haematol* 1995;**54**:163–71.
6. Rapi S, Ermini A, Bartolini L, Caldini A, Del Genovese A, Miele RA, Buggiani A, Fanelli A. Reticulocytes and reticulated platelets: simultaneous measurement in whole blood by flow cytometry. *Clin Chem Lab Med* 1998;**36**:211–14.
7. Takubo T, Yamane T, Hino M, Tsuda I, Tatsumi N. Usefulness of determining reticulated and large platelets in idiopathic thrombocytopenic purpura. *Acta Haematol* 1998;**99**:109–10.
8. Koh KR, Yamane T, Ohta K, Hino M, Takubo T, Tatsumi N. Pathophysiological significance of simultaneous measurement of reticulated platelets, large platelets and serum thrombopoietin in non-neoplastic thrombocytopenic disorders. *Eur J Haematol* 1999;**63**:295–301.
9. Matic GB, Chapman SE, Zaiss M, Rothe G, Schmitz G. Whole blood analysis of reticulated platelets: improvements of detection and assay stability. *Cytometry* 1998;**34**:229–34.
10. Rinder HM, Munz JU, Ault AK, Bonan LJ, Smith RB. Reticulated platelets in the evaluation of thrombopoietic disorders. *Arch Pathol Lab Med* 1993;**117**:606–10.
11. Romp KG, Peters PW, Hoffman M. Reticulated platelet counts in patients undergoing autologous bone marrow transplantation: an aid in assessing marrow recovery. *Am J Hematol* 1994;**46**:319–24.
12. Bonan JL, Rinder MH, Smith RB. Determination of the percentage of thiazole orange (TO)-positive, "reticulated" platelets using autologous erythrocyte TO fluorescence as an internal standard. *Cytometry* 1993;**14**:690–4.
13. Richards EM, Baglin PT. Quantitation of reticulated platelets: methodology and clinical application. *Br J Haematol* 1995;**91**:445–51.
14. Kurata Y, Hayashi S, Kiyoi T, Kosugi S, Kashiwagi H, Honda S, Tomiyama Y. Diagnostic value of tests for reticulated platelets, plasma glycocalicin, and thrombopoietin levels for discriminating between hyperdestructive and hypoplastic thrombocytopenia. *Am J Clin Pathol* 2001;**115**:656–64.
15. Robinson MS, Mackie JI, Khair K, Liesner R, Goodall HA, Savidge FG, Machin JS, Harrison P. Flow cytometric analysis of reticulated platelets: evidence for a large proportion of non-specific labelling of dense granules by fluorescent dyes. *Br J Haematol* 1998;**100**:351–57.
16. Robinson MS, MacKie JI, Machin JS, Harrison P. Two colour analysis of reticulated platelets. *Clin Lab Haematol* 2000;**22**:211–3.
17. Briggs C, Kunka S, Hart D, Oguni S, Machin JS. Assessment of an immature platelet fraction (IPF) in peripheral thrombocytopenia. *Br J Haematol* 2004;**126**:93–9.
18. Abe Y, Wada H, Tomatsu H, *et al.* A simple technique to determine thrombopoiesis level using immature platelet fraction (IPF). *Thromb Res* 2006;**118**:463–9.
19. Takami A, Shibayama M, Orito M, Omote M, Okumura H, Yamashita T, Shimadoi S, Yoshida T, Nakao S, Asakura H. Immature platelet fraction for prediction of platelet engraftment after allogeneic stem cell transplantation. *Bone Marrow Transplant* 2007;**39**:501–7.
20. Zucker ML, Murphy AC, Rachel MJ, Martinez AG, Abhyankar S, McGuirk PJ, Reid JK, Plapp VF. Immature platelet fraction as a predictor of platelet recovery following hematopoietic progenitor cell transplantation. *Lab Hematol* 2006;**12**:125–30.

21. Briggs C, Hart D, Kunka S, Oguni S, Machin JS. Immature platelet fraction measurement: a future guide to platelet transfusion requirement after haematopoietic stem cell transplantation. *Transfus Med* 2006;**16**:101–9.

22. Dolan MM, Singleton PT, Neglia J, Cioc A. Aplastic anemia and monosomy 7-associated dysmegakaryocytopoiesis. *Am J Clin Pathol* 2006;**126**:925–30.

Anti-Moesin Antibodies in the Serum of Patients with Aplastic Anemia Stimulate Peripheral Blood Mononuclear Cells to Secrete TNF-α and IFN-γ[1]

Hiroyuki Takamatsu,[2*†] J. Luis Espinoza,[2*] Xuzhang Lu,[*] Zhirong Qi,[*] Katsuya Okawa,[‡] and Shinji Nakao[3*]

Moesin is an intracellular protein that links the cell membrane and cytoskeleton, while also mediating the formation of microtubules and cell adhesion sites as well as ruffling of the cell membrane. To determine the roles of anti-moesin Abs derived from the serum of patients with aplastic anemia (AA) in the pathophysiology of bone marrow failure, we studied the expression of moesin on various blood cells and the effects of anti-moesin Abs on the moesin-expressing cells. The proteins recognized by anti-moesin mAbs were detectable on the surface of T cells, NK cells, and monocytes from healthy individuals as well as on THP-1 cells. The peptide mass fingerprinting of the THP-1 cell surface protein and the knock-down experiments using short hairpin RNA proved that the protein is moesin itself. Both the anti-moesin mAbs and the anti-moesin polyclonal Abs purified from the AA patients' sera stimulated THP-1 cells and the PBMCs of healthy individuals and AA patients to secrete 60–80% as much TNF-α as did LPS 100 ng/ml. Although the polyclonal Abs induced IFN-γ secretion from the PBMCs of healthy individuals only when the PBMCs were prestimulated by anti-CD3 mAbs, the anti-moesin Abs were capable of inducing IFN-γ secretion from the PBMCs of AA patients by themselves. Anti-moesin Abs may therefore indirectly contribute to the suppression of hematopoiesis in AA patients by inducing myelosuppressive cytokines from immunocompetent cells. ***The Journal of Immunology*****, 2009, 182: 703–710.**

Acquired aplastic anemia (AA)[4] is a syndrome characterized by pancytopenia and bone marrow (BM) hypoplasia (1). The T cell-mediated suppression of hematopoiesis is considered to be the most important mechanism responsible for the development of this syndrome because approximately 70% of AA patients respond to immunosuppressive therapy, such as antithymocyte globulin and cyclosporine (2, 3). In addition to a large body of evidence for T cell involvement in the pathogenesis of AA (4–7), recent studies have revealed the presence of Abs specific to self-Ags in the serum of AA patients (8–11). Although some of these Abs are directed toward Ags that are abundant in hematopoietic cells (e.g., kinectin (Ref. 8) and DRS-1 (Ref. 9)), their roles in the pathophysiology of AA are unclear.

Of the various autoAbs detected in the autoimmune diseases, some are known to exhibit stimulatory effects on the target cells rather than inhibitory effects, such as anti-thyroglobulin Abs in Basedow's disease (12) and anti-desmoglein Abs in pemphigus vulgaris (12, 13). The autoAbs specific to platelet-derived growth factor receptors in patients with scleroderma and those with extensive chronic graft-vs-host diseases trigger an intracellular loop, involving Ha-Ras-ERK 1 and 2 (ERK 1/2)-reactive oxygen species (Ha-Ras-ERK 1/2-ROS), and augment collagen gene expression as well as myofibroblast phenotype conversion of normal human primary fibroblasts (14, 15). The anti-proteinase 3 Abs detected in Wegener's granuloma stimulate monocytes through the binding of cell surface proteinase 3 to secrete IL-8 (16). The autoAbs detected in AA patients may also be involved in the pathophysiology of BM failure by way of other mechanisms than the direct toxicity against the hematopoietic cells, though there has been no evidence for such functional autoAbs in AA patients.

We previously demonstrated that Abs specific to moesin, a membrane-cytoskeleton linker protein in the cytoplasm, were detectable in approximately 40% of AA patients (11). Moesin is an intracellular protein that links the cell membrane and cytoskeleton, and mediates the formation of microtubules and cell adhesion sites as well as ruffling of the cell membrane (17). On the other hand, some reports have identified molecules that were recognized by anti-moesin mAbs on the surface of blood cells such as T cells and macrophages (18, 19). Because these immune cells are an important source of myelosuppressive cytokines such as TNF-α and IFN-γ, it is conceivable that anti-moesin Abs in AA patients may bind such moesin-like molecules on these immune cells and affect the cytokine secretion from these cells.

To test these hypotheses, we studied the expression of moesin on blood cells and the effects of anti-moesin Abs on the moesin-expressing

*Cellular Transplantation Biology, Kanazawa University Graduate School of Medical Science, and †Internal Medicine, NTT WEST Kanazawa Hospital, Kanazawa, Ishikawa, and ‡Biomolecular Characterization Unit, Frontier Technology Center, Kyoto University Graduate School of Medicine, Kyoto, Japan

Received for publication August 28, 2008. Accepted for publication October 22, 2008.

The costs of publication of this article were defrayed in part by the payment of page charges. This article must therefore be hereby marked *advertisement* in accordance with 18 U.S.C. Section 1734 solely to indicate this fact.

[1] This work was supported by a Grant-in-Aid for Scientific Research from the Ministry of Education, Science, Technology, Sports and Culture of Japan (KAKENHI No. 19659243) and grants from the Research Committee for Idiopathic Hematopoietic Disorders, the Ministry of Health, Labor, and Welfare, Japan.

[2] H.T. and J.L.E. contributed equally to this work.

[3] Address correspondence and reprint requests to Dr. Shinji Nakao, Cellular Transplantation Biology, Kanazawa University Graduate School of Medical Science, Kanazawa, Ishikawa 920-8641, Japan. E-mail address: snakao@med3.m.kanazawa-u.ac.jp

[4] Abbreviations used in this paper: AA, aplastic anemia; BM, bone marrow; pAb, polyclonal Ab; PB, peripheral blood.